

Crack formation and tensile stress-crack opening behavior of Fiber Reinforced Cementitious Composites (FRCC)

E.B. Pereira, G. Fischer

Technical University of Denmark, Lyngby, Denmark

J.A.O. Barros

University of Minho, Guimaraes, Portugal

M. Lepech

Stanford University, Palo Alto, U.S.A.

ABSTRACT: The formation and further development of cracking in strain hardening cementitious composites under tensile loading strongly influences their mechanical behavior. The work presented in this paper describes the crack formation in fiber reinforced cement composites (FRCC). The experimental results are analyzed using a digital image analysis technique to gain detailed insight in the cracking process during the propagation and the opening phases under tensile loading. The data and observations obtained from these tests are used to derive the tensile stress-crack opening behavior of different types of FRCC and to analyze and compare the effect of various composite parameters including fiber reinforcement, cementitious matrix, and interfacial bond properties. In the experimental program, the FRCC specimens are notched and tested in direct tension with the purpose of inducing a single crack during testing. Subsequently, the corresponding crack behavior in terms of stress-crack opening for all specimens is derived, allowing a quantitative evaluation of the performance of the different fiber reinforcements. The monitoring of the crack formation with the digital image acquisition allows the identification of the stages of crack development. The comparison of the stage sequences among different tensioned specimens contributes to the qualitative assessment of the bridging effect obtained in each composite system and to the description of the features associated with the singular crack generated during testing.

1 INTRODUCTION

In the perspective of the structural design, strain-hardening ability in tension is often referred to as the most important property of Strain-hardening Cement Composites (SHCC). The spectrum of structural problems, of quasi-static or dynamic nature, which can be effectively solved by using these materials is wide. They also open new fields of innovative structural systems and strengthening techniques.

Under certain circumstances, strain-hardening results in the ability of the material to develop multiple cracks in tension. This relevant material property has, in a simple view, a dual advantage in engineering applications: while much more cracks develop for the same deformation level, the crack opening is much smaller. The resulting benefits in terms of durability and the preservation of functional properties of the structural elements are evident. The higher energy dissipation ability, *per se*, at the level of a single crack is even multiplied by the high number of cracks developed, resulting in a very high toughness material. Engineered Cement Composites (ECC) represent a class of cementitious based materials, typically reinforced with Polyvinyl Alcohol

(PVA) fibers, which was objectively proved to be able to gather these requisites in an efficient manner (Li 2003, Fischer & Li 2007).

For the full use of all the SHCC material potentialities, in the recent past some efforts have been made to develop numerical modeling strategies especially suited to simulate the behavior of SHCC structures (Kabele 2007). These models may be of a continuum nature or not, but in general their performance and accuracy has always to rely on a deep and precise assessment of the material behavior. This usually requires the study of the material at a smaller scale than the structural.

The material behavior of SHCC is a delicate balance of a wide multiplicity of factors. Among others, the main ones are the interfacial bonding and fiber pull-out properties, the relation between the material parameters of the isolated fibers and of the matrix, the variation of the flaw size, the fiber orientation and their distribution in the matrix. The randomness associated to all these parameters also plays an important role in the composite behavior. Adding more complexity to the problem, all these factors interact with each other in a highly coupled fashion. As a result, it is not easy, if not impracticable, to study

them separately or in an uncoupled fashion. In this context, the assessment of the behavior of the SHCC at the level of a single planar crack may represent a valuable strategy to extract the necessary parameters for the mechanical characterization of SHCC, in a modeling or a design perspective. This strategy does not imply the need for a full understanding of all the micro mechanisms happening at the level of the fibers, matrix or interfaces. Consequently, it can provide the relevant information about the material properties of the composite for a precise and correct structural modeling and design with SHCC materials, in an easy to handle fashion. Alternatively, it can also configure an essential tool for the material design process. Some difficulties may emerge, however, when trying to assess the behavior of a single crack experimentally, mainly if the material is specifically designed to develop multiple cracks and demonstrates high tolerance to damage, as is often the case.

In order to produce the adequate mechanical conditions for the emergence and evolution of a single crack, the stress distribution on test specimens needs to be locally changed and intensified. This may be typically achieved by introducing constrictions or notches in some sections of the test specimen (Shah 1996, Fischer et al. 2007). At this scale level, it is important to gather more information about the effect of various composite parameters. The fiber reinforcement, the cementitious matrix and interfacial bond properties can be assessed by observing the stress-crack opening behavior of what may be considered as a single planar crack, at a meso-scale level. Digital imaging systems may represent a valuable contribution for the assessment of these material features. These systems allow the representation of the generated strain fields during testing, with high precision and at small scales. This is typically done by interpolation of the observed displacements from a matrix of dots superimposed to the digital image. The allowable visual magnification determines the scale at which the strengthening mechanisms are studied. The crack appearance and development during tension in notched SHCC specimens can be assessed, particularly in the early stages of the test sequence, while the crack plane fully develops and the tensile stresses acting at the matrix gradually transfer into the fibers bridging the crack.

2 EXPERIMENTAL PROGRAM

In the present work the tensile behavior of six fiber reinforced cementitious composites is assessed. The matrix used was essentially the same for all the composites, while the fiber reinforcement was changed in type, content and nature. This work focuses mainly on the study of the test-setup and the conditions needed to assure that the behavior of a single

crack is accessed as close as possible. Since these materials are desirably designed to develop multiple cracks in tension, the characterization of the mechanical behavior in terms of its tensile stress-crack opening at the level of a single crack is not straightforward and can be troublesome.

The experimental work is composed of two parts. First, the experimental characterization of the tensile stress-crack opening behavior of each composite is carried out. Secondly, giving more focus to the observation of the stages of crack appearance and propagation in tension, cracking is assessed with a digital imaging system. For this last purpose, two different variants of the proposed geometry for the tensile tests were developed. The intention is to allow the visual access and further digital strain field interpolation of the cracking region, which is not possible with the standard four-notched specimens.

2.1 Tensile tests in notched specimens

As reported in previous works (Fischer et al. 2007), the execution of a notch in each of the four faces of the prismatic ECC specimens seems to be satisfactory in assuring the proper shielding and development of a crack inside the notched region. This condition is naturally dependant on the ratio between the first cracking stress and the peak stress. In the present work the geometry adopted to conduct the tensile tests with different fiber reinforced cementitious composites is represented in Figure 1. The adopted dimensions allow the reduction of the specimen's cross section to 40% of its initial value, within a total extension of 0.5 mm, the notch thickness. The very small notch thickness was adopted with the intention of isolating, as much as possible, one single planar crack.

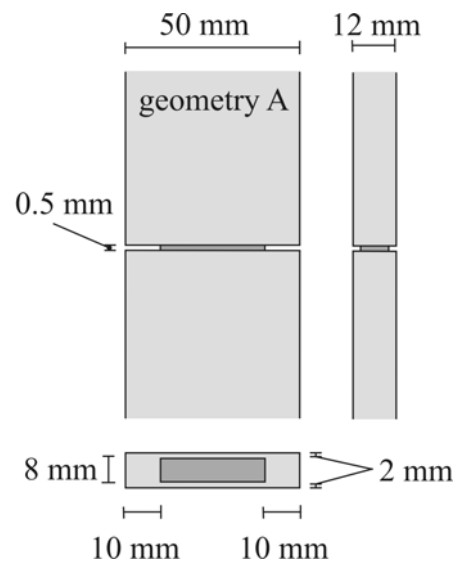


Figure 1. Schematic representation of the specimen geometry A, adopted for the experimental assessment of the tensile behavior of FRCC. The specimen's length was 120.0 mm.

Elongated plates of 60 cm long, 10.5 cm wide and 1.6 cm thick were cast and left to dry cure for 28 days. From each of these plates the specimens were cut in the longitudinal direction and the casting free surface was rectified. The matrix composition was similar in all of them, and the weight proportions of the ingredients are represented in table 1.

Table 1. Weight proportions of the matrix constituents.

Cement	Fly ash	Fine sand	Quartz powder
1	2	0.35	0.35

Fibers of two different natures were used: PVA (polyvinyl alcohol) based and PAN (polyacrylnitrile) based. The main geometrical and mechanical properties of these fibers are presented in table 2.

Table 2. Main properties of the fibers studied.

Fiber	Abbrev.	Tensile strength	Length	Diameter
		MPa	mm	μm
PVA Rec 15	PVA	1600	8	40.0
PAN D10 1.5	PAN 1.5	826	6	12.7
PAN D10 3.0	PAN 3.0	767	6	18.0
PAN D18 6.7	PAN 6.7	413	6	26.8
PAN D18 30	PAN 30	295	6	57.0

For the PAN fibers all the mixes contained 2% of fibers in volume, while for PVA fibers 1% and 2% volume amounts were used.

The test sequence consisted of submitting the specimens to a displacement controlled constant axial extension rate of $5 \mu\text{m/s}$. This deformation rate was transmitted from the hydraulic actuator to the specimen by means of two hydraulic grips. These grips conferred fixed support to the specimen's ends (rotations and transverse displacements were blocked). While testing, the opening of the notch was evaluated by means of two clip gages, positioned in opposite sides as shown in Figure 2.

2.2 Optical monitoring of crack development

The cracking mechanisms taking place inside fiber reinforced cement composites manifest themselves visually when these cracks either reach or initiate at the surface of the specimens. The monitoring of these mechanisms at a meso-scale level may provide important information about the interaction between the fibers and the matrix, with a special focus on the strengthening mechanisms and on the cracking stages and crack development.

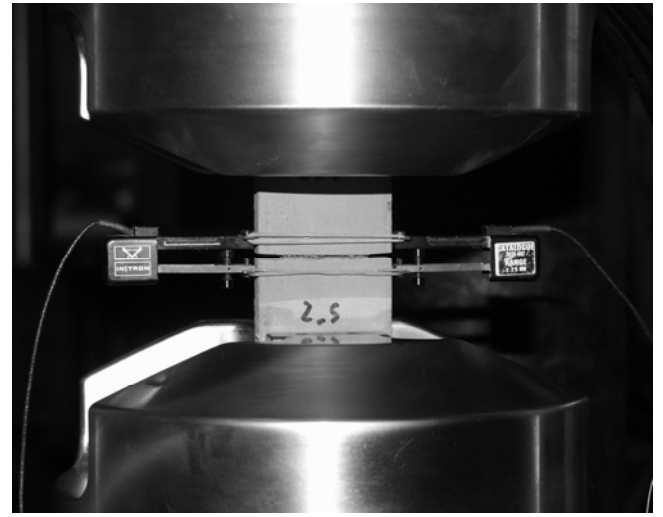


Figure 2. Picture of the test-setup used for the tensile behavior assessment of the FRCC, showing the specimen fixed in the extremities by the hydraulic grips and the two clip gages used to monitor the crack opening.

The monitoring of crack appearance and progression during testing with the optical system requires the existence of a smooth and visually accessible surface in one of the specimen's faces, which is incompatible with the slim grooves used in geometry A (Fig.1). The small scale at which the observations are supposed to be carried out implies also the need of adopting very small apertures in the optical lenses to maximize the depth of field, which in turn demands for extra lighting. These requirements impose a delicate balance of specimen's shape, lighting conditions and the precision of the measurements. For this purpose, in the present work two distinct specimen shapes were conceived specifically for the study of crack development with the optical system (see Fig. 3).

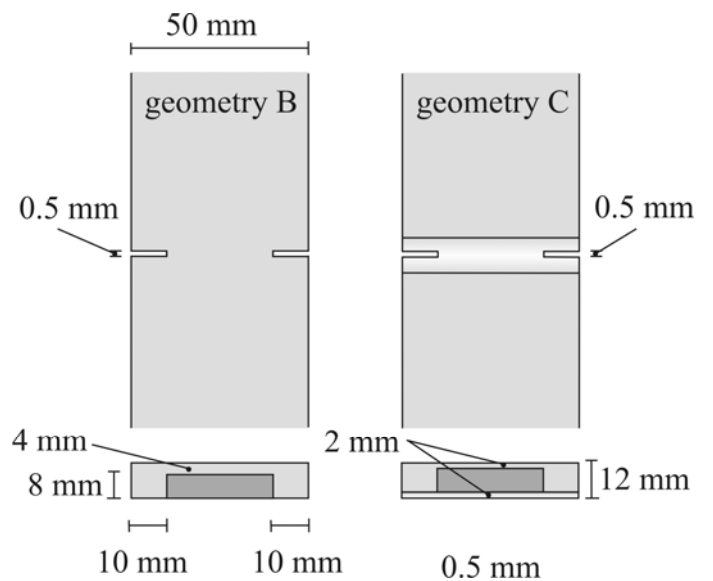


Figure 3. Geometries adopted for the visual inspection and optical monitoring of the FRCC specimens. Geometry B provides a flat surface and the geometry C tries to replicate the same conditions obtained with the shape used for tensile tests, the geometry A. The specimens' length was 120.0 mm.

One of the proposed solutions consists on simply suppressing one of the notches, keeping the same shape and dimensions of the notched cross-section area. This is achieved by executing the two 10 mm depth notches, one in each of the opposite smaller sides, and one 4 mm depth slit along one of the longer sides, as represented in Figure 3 (geometry B). In this fashion, one of the specimen's faces is kept flat in the notched region. The original pre-cracked stress field in the notched area is, nevertheless, changed when compared with the one induced by geometry A. However, the flat surface is the most favorable for the optical monitoring.

The other geometry proposed consisted on creating a round cylindrical surface replacing one of the slits (geometry C, see Figs. 3 and 4). This procedure tries to replicate, as close as possible, the stress fields generated near the notched area by replacing the discrete notch with a cylindrical smooth surface with 22 mm of diameter. This cylindrical surface reaches a depth of 2 mm, the same as the original discrete notch. In this case the intention is to achieve the best compromise between the flatness and smoothness required for a precise digital interpolation of the deformations, while keeping the local strong constriction necessary to intensify the stress field adequately. At the same time, while allowing the visual access of the crack propagation, the proposed shape approximately preserves the axial centering of the tensile loading (Fig. 4).



Figure 4. Picture of one of the specimens conceived with the geometry C, allowing the visual inspection of crack development and the preservation, as close as possible, of the notched cross section.

3 RESULTS AND DISCUSSION

3.1 Tensile tests

The obtained results in terms of tensile stress *versus* crack mouth opening displacement (CMOD) for the six different composites are shown in Figure 5.

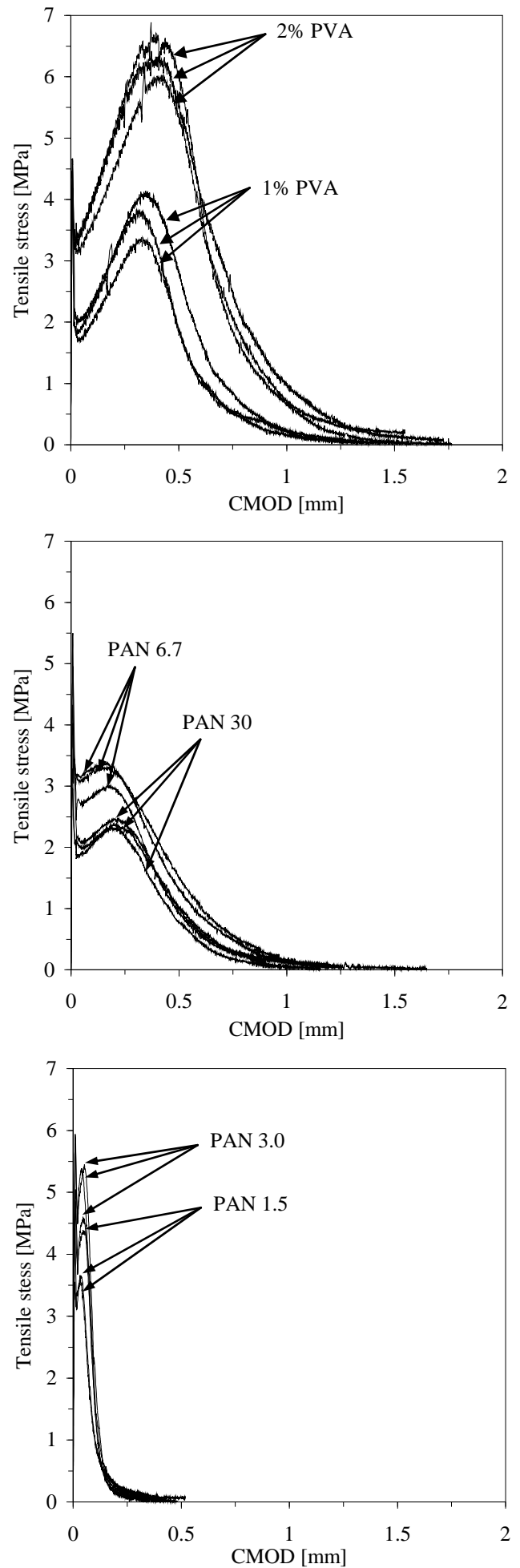


Figure 5. Graphics showing the obtained tensile stress *versus* CMOD curves for the six tested FRCC.

The tensile stress values result from the normalization of the tensile load with respect to the notched cross sectional area. For clarity, only the results of three specimens are shown for each composite. The anomalous results were also excluded.

In general, the first pertinent observation about the obtained results is that, for each composite, there is a good agreement between curves obtained from different specimens. The scatter of results may change with the procedure used to cast the specimens, due to differently induced fiber distributions and predominant orientations. Excluding this factor, one may say that the true character of the material behavior in tension is captured by this type of test-setup. It is clear that parameters like the nature, the geometrical and the mechanical properties of the used fibers play an important role in the observed features of the tensile behavior of each composite. The direct correlation between them and the final composite tensile behavior is not easily accessible, as generally recognized. However, each of the presented stress *vs* CMOD curves is apparently able to reveal the role that the geometrical and mechanical properties of the fibers have in the overall tensile behavior of the composite.

The obtained results seem to reveal some few distinct generic stages of a typical mechanical behavior.

At the onset of tensile testing, the evolution starts with what can be assumed as a predominantly elastic behavior, with a very steep increase of load bearing capacity while tensile deformation increases. This first stage may be assumed to end when the matrix cracking strength is achieved, with a very quick transition of the tensile stresses from the cracked matrix to the fibers. Preliminary stages of micro-cracking and micro-defect propagation may affect the shape of this transition stage, ruled mainly by fracture mechanisms and eventually dependent of micro-defect shape and size.

In a second stage, the internal readjustment of the composite microstructure to the new damaged configuration typically reveals itself by the subsequently observed sharp load decay. Factors like fiber-matrix bonding, fiber diameter, number of fibers bridging the crack and the ratio between the Young's modulus of fibers and the bulk matrix may play an important role.

The former is followed by a new hardening stage, most likely supported by the full mobilization of the fiber-matrix bonding mechanisms and while fibers stretch. The peak stress is reached in this third stage, when the stiffening effect of the fiber reinforcement is exhausted either due to fiber debonding or fiber rupture predominance.

The fourth and last stage consists of the last softening branch observed in all curves. It coincides with the gradual neutralization of the remaining bonds between the opposite crack faces.

This is obviously a simplistic interpretation of the complex mechanisms taking place at the level of a crack in the bulk composite, but somehow they summarize and condense in a rational and easy to handle approach the tensile behavior of FRCC, very useful in a design perspective.

Observing Figure 5, it becomes clear that a strong correlation can be established between the geometrical and mechanical properties of the used fibers and the features of the stages previously described. Without detailing too much the micromechanical aspects of each fiber reinforcement type, what is relevant in the present context is to stress the importance of the shape, size, magnitude and significance of each of the identified stages in the overall assessed tensile behavior. These will reveal themselves in a particular way when the material is used in a structure. One brief example would be the ability of the material to develop multiple cracks in tension, roughly dependant on the ratio between first cracking stress (first stage) and the peak bridging stress (third stage). Another example would be the durability and functional design aspects, very dependent on crack opening, which is most likely correlated with the inclination of the second stage hardening branch.

The sequence of distinctive stages above mentioned seems to be clearly identifiable in all the tested composites. The adopted fiber reinforcements reveal different mechanical performances in tension, but still these stages remain clearly distinctive and keep the same formal details. This suggests that a rational design approach can be based on the assumption that, in general, the stress-crack opening behavior of FRCC follows a standard sequence of stages assuming the shape of a generic design tensile stress-crack opening curve (Fig.6).

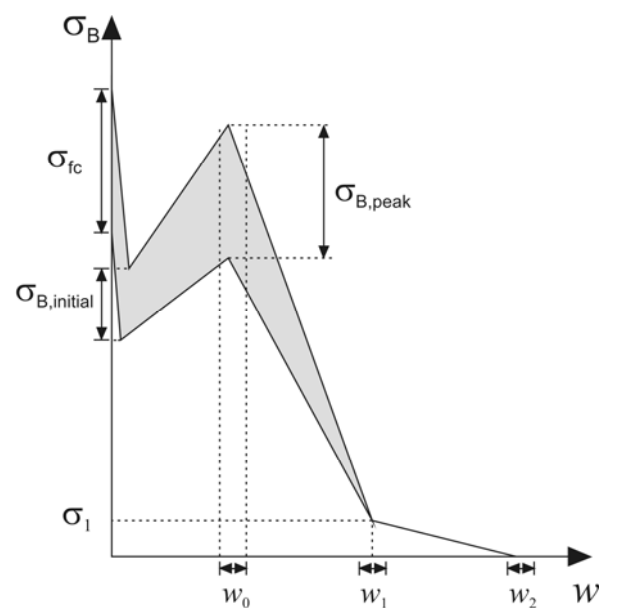


Figure 6. Diagram representing the generic bridging stress (σ_B) versus crack opening (w) relationship, typical of FRCC.

As previously reported (Fischer et al. 2007), the simplification of this behavior by a tri-linear curve may enclose all the necessary and fundamental details for the overall composite tensile behavior. One plausible way to represent it would be as shown in Figure 6, where the first branch may be suppressed for further simplification.

The identification of the parameters that define the shape of the bridging stress, σ_B , versus the crack opening, w relationship may be done experimentally. For that purpose the above suggested setup conditions may be adopted. The first cracking strength, σ_{fc} , the initial bridging stress, $\sigma_{B,initial}$, the peak bridging stress, $\sigma_{B,peak}$, and the corresponding crack opening at peak bridging stress, w_0 , represent the most significant parameters to be identified. Subsequently there is the residual bridging stress, σ_1 , the corresponding crack opening, w_1 , and finally the ultimate cohesive crack opening, w_2 . All these data, and the scatter associated to each parameter, may be used to support the structural design and to define safety factors for each mechanical parameter. Alternatively, in some cases the material requisites may be imposed by the structural concept. These requisites may assume the shape of a predetermined bridging stress-crack opening curve, which will constitute the support of the material design task with a FRCC based solution. In this fashion, material and structural design may be integrated.

3.2 Crack development under tension

The collection of photos taken during tensile testing of the specimens with geometry C was used to digitally interpolate the strain fields near the notched region. The point matrix used to interpolate the strain fields was discretized with enough accuracy to make possible the identification of even invisible cracks, with openings smaller than 0.1 mm. The test procedure was the same as previously referred.

The sequence of pictures shown in Figure 7 represents, in gray scale, the strain fields obtained in five specific stages of the tensile testing. Stage zero refers to the onset of the test sequence, with the specimen still unloaded. The white dots reflect unidentifiable regions of the specimen's surface, mainly constituted by pores with deficient illumination and excessive geometric gradients. The represented strain fields are useful to support the interpretation of the cracking process observed in the composite, but only in a qualitative perspective. They represent a convenient way to visualize and interpret the discrete displacements observed in all the sampling points, using a reference length of 15 pixels.

Among all the tests preformed, the evolution of cracking of the composite reinforced with 2% of PVA fibers was selected (Fig. 7), due to its greater potential to develop multiple cracks.

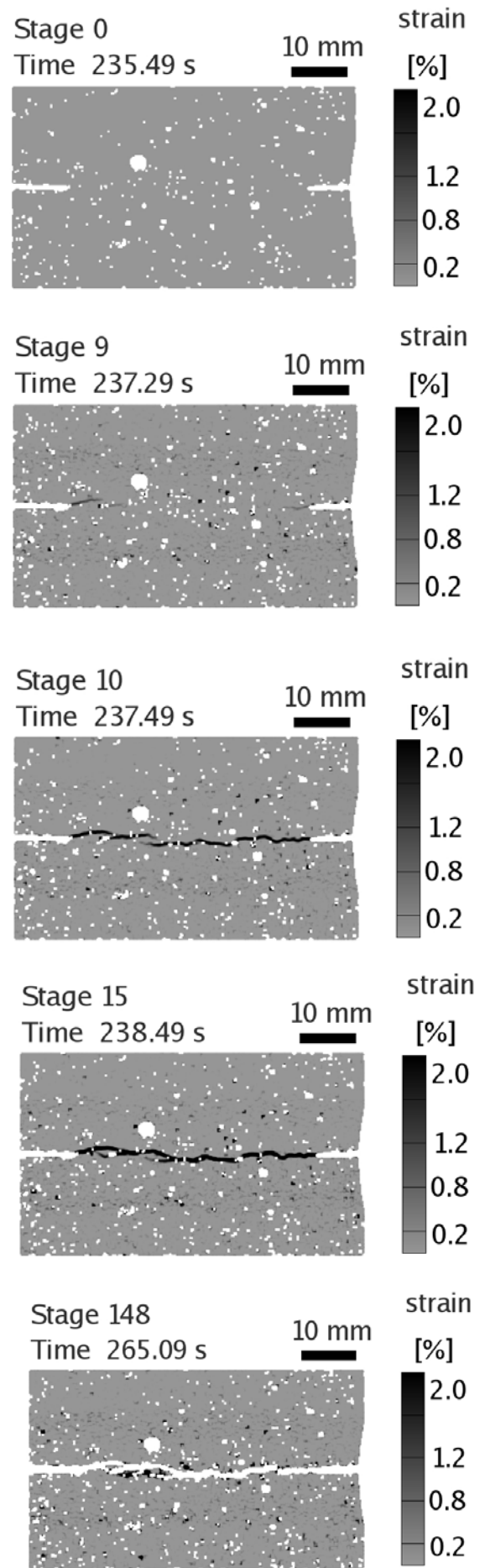


Figure 7. Pictures of the composite containing 2% of PVA and adopting geometry C, with the corresponding interpolated strain pattern superimposed. Stage zero corresponds to the reference stage, unloaded and undeformed.

The selected sequence of five pictures tries to summarize the most important stages of the overall cracking process evolution observed in the notched specimens. First of all, it is important to refer that the CMOD measured during all testing in the opposite notches was approximately the same (less than 0.001 mm of difference). This was expectable, nonetheless a confirmation is essential to assure that the prescribed boundary conditions are in fact being effectively accomplished, giving the sensitivity of the test. It may be assumed then that the displacement is taking place exclusively in the direction perpendicular to the notched plane.

Observing the sequence of pictures in Figure 7, it is apparent that the presence of the notches induces the appearance and propagation of what may be considered as a single crack. Looking at Stage 9, close to the mouth of the left and right notches it is visible the appearance of small regions where high strain gradients are detected, already taking the shape of a preliminary crack. It is not possible to visualize any discrete crack with naked eye or even with high magnifications (up to 10 times), so these preliminary small strain concentration regions assume eventually the shape of a damaged region of material which in further stages will originate the discrete crack.

As shown in Stage 10, only 0.2 seconds after the Stage 9, the visible areas of high gradients in the strain field are now spread through the entire specimen's width, closely aligned and assuming the shape of a future tension crack. It is still not possible to visualize a discrete crack in the specimen's surface, but the strain gradients are very localized and confined to a thin aligned region. Stages 9 and 10 correspond to the right after and right before peak cracking stress reaching, respectively.

At Stage 15 the crack is apparently fully developed. From here, there is a constant increase of the load carrying capacity of the specimen with the gradual increase of the spacing between the opposite crack mouth faces. The dark continuous line connecting both notches represents the region where strong strain gradients are observed, most likely the tensile crack, already fully developed.

The last stage represented is the Stage 148, which corresponds to the instant when the peak bridging stress is reached. The white line separating the two regions of the specimen reveals that the strain gradients in that region are already too high to be computed, so one may assume that a completely discrete crack is opening.

In Figure 8 the same stage of the tensile test for the same composite is shown, this time adopting the geometry B. The interpolated strain fields were not superimposed to the photo, since the cracking pattern attained when the peak bridging stress was reached is clear enough. It may be observed that the geometry B does not create the conditions for the appearance and propagation of a single crack, and

the high potential of the composite for the generation of multiple cracks is consequently revealed. This is the kind of situation that is not desirable for the characterization of the stress-crack opening behavior of FRCC. The pronounced crack branching and crack multiplication increases the resulting axial deformation for the same load level, when compared with the situation where a single crack is present. At the same time, the behavior of several small parallel cracks opening simultaneously, most likely in different stages of its stress-crack opening diagram, masks the true character of the stress - crack opening behavior of the assumed single crack. These features are relevant in a material design perspective, and for their clear and unmasked experimental characterization the isolation of a single crack should be attained as close as possible. For that purpose, the execution of the four notches assuming the configuration adopted in geometry A (see Fig. 1) is decisive.



Figure 8. Picture of the composite containing 2% of PVA adopting geometry B, at the instant when the peak bridging stress is reached.

The results obtained with geometry B revealed themselves very useful in the understanding of the cracking behavior of the studied composites. The appearance of parallel cracks and their interaction, their chronology and the differences observed in these features between different composites inputs also qualitative information of great value. All this data is, though, extensive and falls out of the scope of the present work. The geometry B allows confining the crack processes to a much smaller area, making easier their observation with small scale high precision optical systems.

Going back to geometry C, with increased magnification it is possible to observe with more detail what happens close to the lateral notches. The small regions where high strain gradients were first detected, at Stage 9 (see Fig. 7), may be studied with more detail. At the same time, a closer insight to the

crack initiation and propagation in the notched region is also allowed, necessary to discern the discrete character of the formed crack.

In Figure 9 the sequence of the most relevant stages of cracking are identified on the stress-CMOD diagram obtained from the tensile test. For clarity, the results are shown only up to a measured value of the CMOD of 1 mm. The series of stages shown was selected in order to represent the most important features detected during the hole testing sequence.

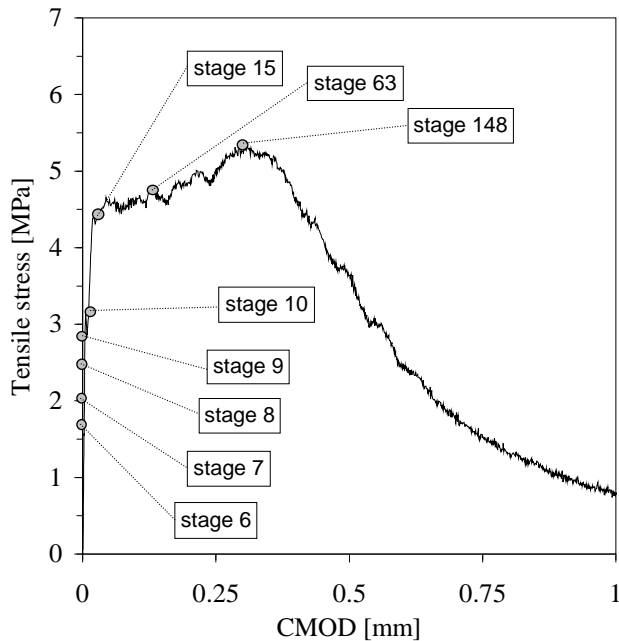


Figure 9. Identification of the relevant stages on the stress – CMOD diagram obtained with geometry C specimen.

The represented stages (Fig. 9) are revealed in Figure 10, where the notch in the right hand part of the specimen was magnified. For each stage, the true photo is presented in the left hand side and the interpolated strain field is shown in the right hand side.

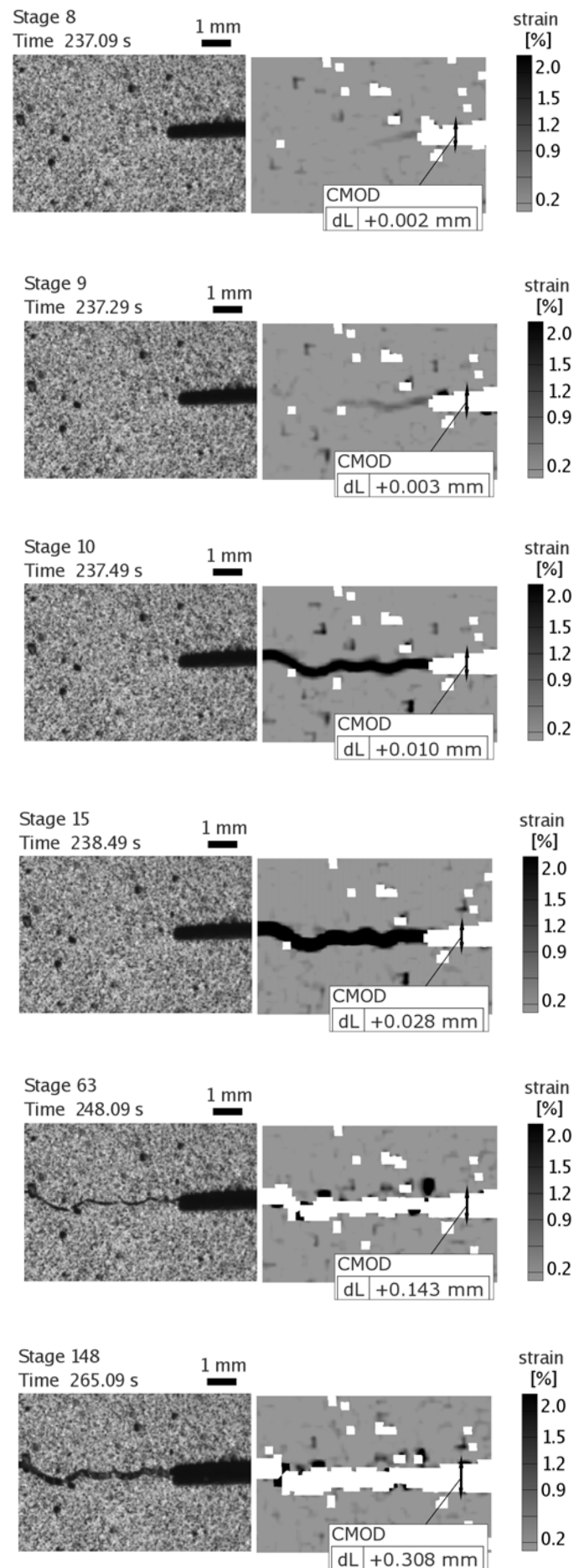
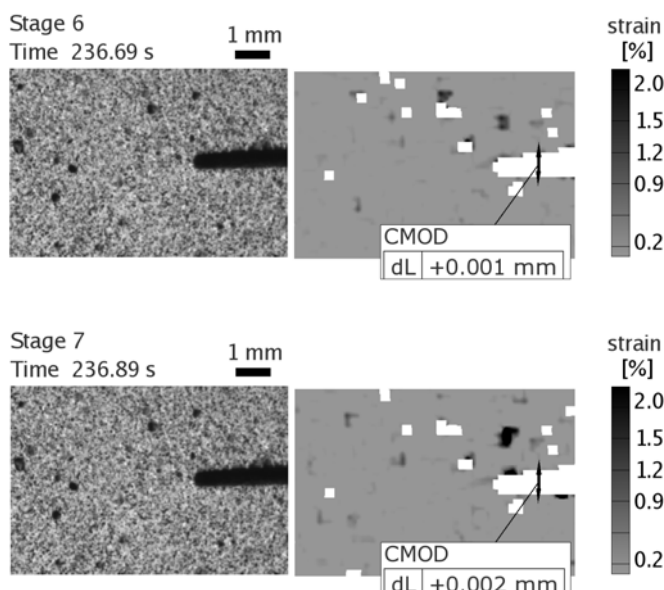


Figure 10. Identification of the relevant stages on the stress – CMOD diagram obtained with geometry C specimen.

By observing Figures 9 and 10 it is possible to follow the initiation and further propagation of the tensile crack. It is also possible to observe that the eventually formed crack is rather invisible up to the Stage 15. However, in this stage the interpolated strain field reveals already a quite clear and pronounced region of intense strain gradient concentration, with the shape of a continuous thin line. This line tracks already the future crack. The interpolated strain field reveals itself very useful on identifying the preliminary stages of the crack formation. The used scale is not small enough to state something conclusive about the cracking processing zone, but the sequence of stages from 6 to 10 (see Fig. 9) seems to indicate that, in the present situation, it may assume a sharp, thin and elongated shape. This was expectable, and agrees with the observations of other researchers (Bolander Jr. & Hikosaka 1995, Otsuka & Date 2000).

In Figure 11 the crack patterns obtained from the tensile testing of dogbone shaped specimens is shown. In Figure 11.a the presented photograph reveals the crack pattern observable in a dogbone surface right before localization and rupture. In Figure 11.b the interpolated strain field obtained using the digital imaging system is superimposed to the original specimen's photo, allowing the observation of the cracking processes at much earlier stages (Lárusson et al. 2009). The results obtained from the tensile testing of several ECC specimens reveal that, in general, following a preliminary stage of elastic behavior a pronounced cracking stage with strain hardening takes place. This stage typically ends with localization for a limit strain of around 4%, after the full development of a system of closely parallel cracks along the longitudinal axis (Lárusson et al. 2009).

The numerical modeling carried out in previous works (Fischer et al. 2007) showed that the tensile stress-strain behavior of these dogbones may be obtained from the stress-crack opening behavior of a single crack. The structural behavior will be mainly the result of the sum of the mechanical behavior encountered at the level of each single crack. The uniaxial character of the stress-CMOD law derived from experimental testing was considered as a non-linear spring. The overall behavior of the dogbone consisted, in this fashion, of the association in series of spring elements representing either the non-linear behavior of each crack or the linear elastic behavior of the intact material between cracks. Additionally, a statistical approach was considered to account for the randomness associated with the material and mechanical properties, in particular the matrix tensile cracking stress.

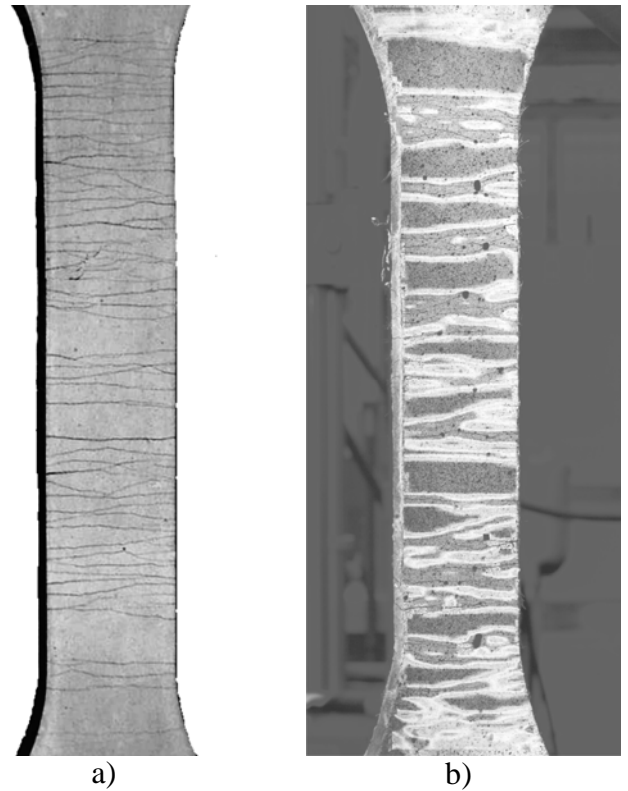


Figure 11. Pictures showing the cracked pattern obtained from the tensile test of two dogbone shaped ECC specimens, exhibiting a system of closely parallel cracks along the longitudinal axis. a) Photo of the specimen right before the peak strength is reached and b) strain field obtained with the digital imaging system (Lárusson et al. 2009).

4 CONCLUSIONS

In the present work the cracking process of notched tensile specimens of FRCC was experimentally assessed. The distinct fibers used as reinforcement of the composites revealed very distinct stress-crack opening behaviors. It is possible, however, to assume that a typical sequence of characteristic stages took place in all the performed tests. The particular features of each stage, such as its magnitude, duration and significance are the reflex of a complex collection of micromechanical mechanisms taking place. These are determined by the matrix, the fibers' properties and their interaction. They may constitute very important information for supporting the design, either of the material itself or of the structure where the material is meant to be used. The proposed curve to describe the tensile behavior of a single crack in FRCC assumes a simple and convenient format, consequently representing an eventually useful instrument to be included in a design strategy for this type of materials.

The isolation of a single crack during tensile testing is an important premise for the truth assessment of the composite mechanical behavior. The high potential of multiple crack development revealed by SHCC is deleterious to that purpose. The local in-

tensification of the stress field achieved by executing the four notches in the specimens, following the aforementioned geometry A, revealed to be a valid strategy to gather the conditions for the formation and propagation of a meso-scopic single crack during tensile tests.

The geometry A did not allow the visual access to the inner cracking region, consequently the geometries B and C were developed. The observations made with the specimen's geometry C allowed to infer that the development of a single crack is, in a meso-scopic perspective, efficiently achieved for the level of the bridging stresses in study. The tensile stress – crack opening curves obtained by using specimen's geometry A may constitute an important element in both the material and the structural design activities. The behavior of a single crack is captured in a simple and appealing way, providing the designer with the most relevant features of the mechanical behavior of the material.

The digital interpolation of the strain fields in specimens' geometries B and C allowed the identification of the features of the most relevant cracking stages. The initiation of the crack at the notches and its subsequent development always in symmetric conditions in terms of deformations sustains the fact that the test setup, particularly the support conditions, was adequate in assuring the initiation and propagation of one planar crack.

5 ACKNOWLEDGMENTS

The first author wishes to thank the Portuguese National Science Foundation for the financial support, through grant SFRH / BD / 36515 / 2007, funded by POPH - QREN, the Social European Fund and the MCTES.

6 REFERENCES

- Bolander Jr, J. & Hikosaka, H., 1995. Simulation of Fracture in Cement-based Composites, *Cem. & Conc. Comp.*, 17: 135-145.
- Fischer, G. & Li, V.C., 2007. Effect of fiber reinforcement on the response of structural members, *Eng. Frac. Mech.*, 74: 258-272.
- Fischer, G., Stang, H. & Dick-Nielsen, L. 2007. Initiation and development of cracking in ECC materials: Experimental observations and modeling. In G. F. A. Carpinteri, P. Gambarova & G. P. (eds.), *High Performance Concrete, Brick-Masonry and Environmental Aspects; Proc. int. symp.*, Vol. 3, *la-FraMCos*. Taylor & Francis, pp. 1517–1522.
- Kabele, P., 2007. Multiscale framework for modeling of fracture in high performance fiber reinforced cementitious composites, *Eng. Frac. Mech.*, 74: 194-209.
- Lárusson, L.H., Fischer, G. & Jönsson, J., 2010. Mechanical interaction of Engineered Cementitious Composite (ECC) reinforced with Fiber Reinforced Polymer (FRP) rebar in

- tensile loading. In G. P. A. G. van Zijl & W. P. Boshoff (eds.) *Advances in Cement-based Materials (ACM2009); Proc. int. symp.*, South Africa, CRC Press/ Balkema.
- Li, V.C., 2003. On Engineered Cementitious Composites (ECC) - A Review of the Material and Its Applications, *J. Adv. Conc. Tech.*, 1 (3): 215-230.
- Otsuka, K. & Date, H., 2000. Fracture process zone in concrete tension specimen, *J. Eng. Frac. Mech.*, 65: 111-131.
- Shah, S.P. et al., 1996. Toughness characterization and toughening mechanisms. In Naaman, A.E. & Reinhardt, H.W. (eds.). *High performance fiber reinforced cement composites 2; Proc. Int. symp.*, E & FN Spon, London.